Pyridoxamine, A Scavenger Agent of Carbohydrates

MIQUEL ADROVER, BARTOLOMÉ VILANOVA, FRANCISCO MUÑOZ, JOSEFA DONOSO

Institut Universitari d'Investigació en Ciències de la Salut (IUNICS), *Departament de Química*, *Universitat de les Illes Balears*, E-07122 *Palma de Mallorca*, *Spain*

Received 5 June 2006; revised 10 October 2006; accepted 13 October 2006

DOI 10.1002/kin.20223
Published online in Wiley InterScience (www.interscience.wiley.com).

ABSTRACT: Pyridoxamine has been found to inhibit protein glycation and to avoid the formation of advanced glycation end-products (AGEs). One of the mechanisms by which pyridoxamine can inhibit glycation involves the scavenger of carbonyl groups with glycation capacity. In this work, we conducted a kinetic study of the reactions of pyridoxamine with various carbohydrates under physiological pH and temperature. The reactions involving hexoses were found to give a tricyclic compound (**5**) in addition to pyridoxal and pyridoxine. Such a tricyclic compound inhibits the Amadori rearrangement and the formation of other carbonyl compounds with glycating properties. The reactions involving pentoses gave compound **7** and pyridoxal—by transamination of the Schiff base. The transamination reaction enhances the inhibitory action of pyridoxamine. The formation rate constants for the Schiff base, k_3, were found to be similar to those for the reactions of D-glucose with amino acids, which suggests competition between pyridoxamine and terminal amino residues in proteins for glycating sites in sugars. These constants are dependent on the electrophilic character of the carbonyl carbon in the carbohydrate.
 Int J Chem Kinet 39: 154–167, 2007

INTRODUCTION

The reaction between amino acids and sugars was first reported by Maillard [1] and was supposed to be the cause of the formation of colored compounds during the cooking of food. However, it was not until 1949 that Sattler reported the end-products of the reaction to be toxic [2]. Subsequently, the process was found to also occur in biological processes, named as a nonenzymatic glycation of proteins [3,4], and was found to be associated with various diseases.

As can be seen in Scheme 1, the first step in a nonenzymatic glycation process is a reversible reaction between the terminal amino residues in the protein and the carbonyl group in the extended form of the sugar (or a sugar derivative) that leads to the formation of a Schiff base. The Schiff base is stable for a limited time after which it undergoes internal rearrangement to a more stable, ketoamine product: an Amadori compound [5]. The Amadori compound in turn can undergo various complex transformations including oxidative decomposition, rearrangement, condensation, and fragmentation that ultimately produce advanced glycation end-products (AGEs) in an irreversible manner [6].

By oxidation, the sugars, the Schiff base, and/or the Amadori compound can form AGE precursors and radical species accelerating the glycation process. The formation of AGEs involves structural and functional changes in proteins. Several studies have shown that changes in protein structure by the effect of the formation of AGEs are behind the development of various pathologies associated with hyperglycemia (e.g., Alzheimer's disease [7], arteriosclerosis [8], cataracts [9], and kidney disorders [10]).

Correspondence to: Bartolomé Vilanova; e-mail: bartomeu.vilanova@uib.es.
Contract grant sponsor: DGICYT.
Contract grant number: CTQ 2005-00250.

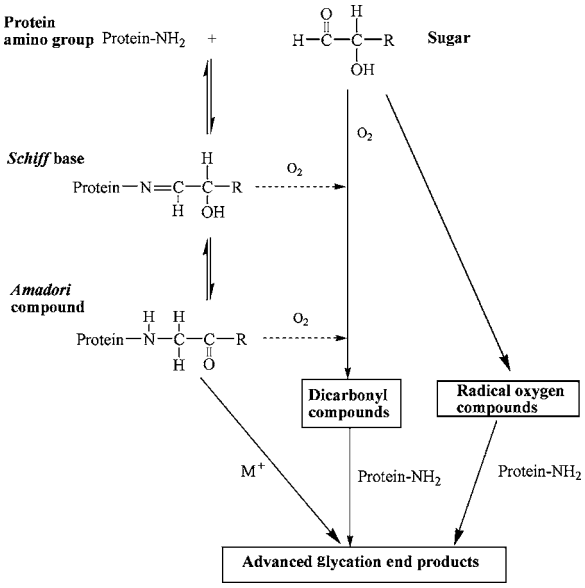

Scheme 1

The chemical nature of AGEs depends on those of the parent glycating carbohydrate and the protein residue. Thus glucosepane [11], which is deemed the most important AGE, and crossline [12] come from hexoses, whereas vesperlysine [9] comes from pentoses. The dimers GOLD, GOLA, and MOLD are only formed with glyoxal or methylglyoxal—both of which result from the decomposition of hexoses [13]—as the glycating agent. On the other hand, pentosidine [14] results from the interaction of arginine and lysine with pentoses (usually D-arabinose or D-ribose) and hexoses. By contrast, the nature of some AGEs is independent of those of the sugar and protein; thus, N^{ε}-(carboxymethyl)lysine (CML) results from the oxidative degradation of the Amadori compound [15] formed between lysine and an aldose, and K2P, which was recently detected in retinal proteins [16], forms whatever the nature of the parent sugar.

In addition, glycation in hyperglycemic patients has been found to involve nucleotides and alter DNA patterns in a way dependent on the individual's age and also to induce congenital abnormalities in children of diabetic mothers [17]. Likewise, proteins can be altered through lipoxidation when the oxidant is a lipid, in which case the resulting products are advanced lipoxidation end-products (ALEs) [18].

The glycation process has been the subject of much research aimed at unraveling its chemical mechanism [19–22]. So far, most studies have focused on the formation of the Schiff base (particularly on those formed by various amino acids and proteins with glucose, which is the sugar most frequently involved in glycation processes). These reactions have been widely examined in kinetic terms [19–21] and revealed that most terminal amino residues have a similar affinity for a given glycating species. Other kinetic studies have examined the hemoglobin glycating properties of various carbohydrates [22].

Most current research in this field is aimed at finding inhibitors of the AGEs formation in order to restrict their accumulation on proteins. The first such potential inhibitors to be studied were aminoguanidine [23] and carnosine [24], which were found to effectively scavenge glycating carbonyl groups. Subsequent studies examined species, such as vitamin C and pyridoxine, which can chelate metal ions acting as catalysts for the electron transfer involved in the formation of AGEs [25]. Work by Hudson and coworkers [26–29] showed that pyridoxamine (one of the six natural vitamers of vitamin B_6) is a powerful in vivo and in vitro inhibitor for AGEs formation. Onorato and coworkers [30] showed that pyridoxamine can also inhibit ALEs formation. The inhibitory action of pyridoxamine may be exerted by (a) inhibiting the oxidation of the Amadori compound via chelation of the metal ions that catalyze it [29]; (b) scavenging carbonyl compounds with glycating properties [26] such as D-glucose or its autoxidation products (glyoxal and glycoaldehyde) [27]; and (c) scavenging oxygen radicals by donating the hydrogen atom of the phenol group in pyridoxamine [26]. Recently, a new generation of pyridoxamine derivatives including dmaPM, diPM [25], and BST-4997 [31] has been found to exhibit enhanced inhibitory properties in various in vivo tests.

There have been virtually no kinetic studies on the interactions between pyridoxamine and sugars. In previous work [32], our group studied the kinetics of the interaction between pyridoxamine and D-glucose in a physiological pH and temperature and detected a tricyclic compound (**5** in Scheme 2) as the main reaction product; such a product precluded the formation of other carbonyl sites with glycating properties from the Schiff base. In addition, compound **5** decomposed into pyridoxal and pyridoxine, which proved capable of inhibiting glycation via other mechanisms [25,28].

In this work, we conducted a kinetic study under physiological pH and temperature of the reaction of pyridoxamine with various aldoses (hexoses and pentoses), some of them play a central role in the formation of AGEs. Major reaction products were isolated, identified, and compared with those resulting from the interaction between pyridoxamine and D-glucose. Based on the results, a general kinetic mechanism for the interaction of pyridoxamine with hexoses and pentoses is proposed, and the kinetic constants of which are determined. The experimental results were validated

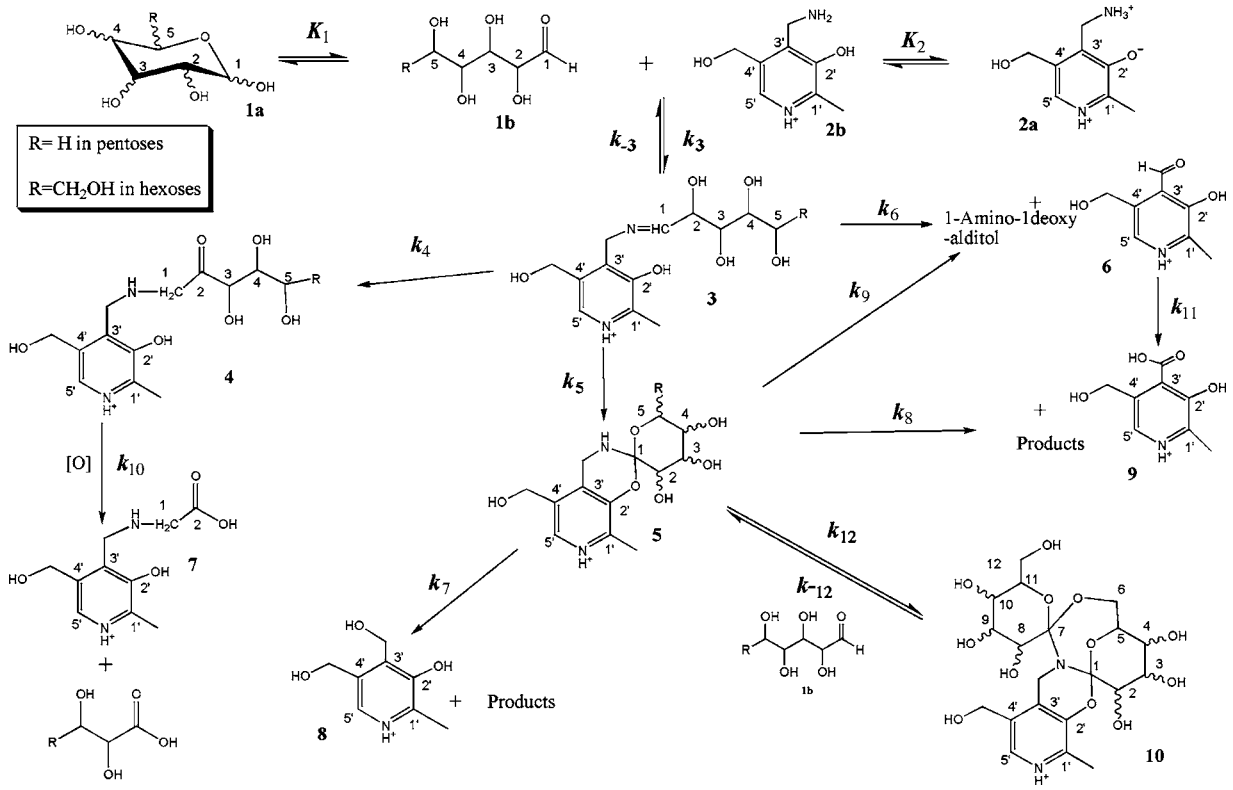

Scheme 2

by calculating the net natural bond orbital (NBO) charge on the carbonyl carbon in the extended forms of the aldoses using the B3LYP functional in conjunction with the 6-31+G* basis set.

EXPERIMENTAL

Material

D-Arabinose, D-lyxose, D-mannose, D-ribose, D-glucose, D-xylose, pyridoxamine (**2**), pyridoxal (**6**), pyridoxine (**8**), 4-pyridoxic acid (**9**), and D_2O (99.9% D) were purchased from Sigma-Aldrich Co. (Madrid, Spain); and D-allose, D-altrose, D-galactose, D-gulose, and D-talose were obtained from Acros Organics (Geel, Belgium) (see Structural formulae 1). All were used as received. The buffering material was reagent grade, and freshly boiled distilled water was used throughout. Reaction kinetics was studied by monitoring changes in HPLC peak area for compounds **2, 5, 6, 7, 8, 9**, and **10** at 321 nm. Pyridoxamine and carbohydrates were used at a concentration of 0.005 and 0.2 M, respectively. The reaction mixture was buffered at pH 7.4 with a 0.5 M phosphate solution and kept at 37°C. Sodium azide at a 0.02% concentration was employed to prevent bacterial growth.

High-Performance Liquid Chromatography

High-performance liquid chromatography (HPLC) analyses were conducted on a Shimadzu-LC 10AT chromatograph equipped with a Rheodyne 7725i universal injector and a Shimadzu SPD-M6A UV/Vis photodiode array detector. The column was a Tracer Excel 120 ODSB model (25×0.46 cm, 5 μm). A gradient of MeCN/water-50 mM potassium phosphate (pH 6.0) was used to separate the target compounds.

NMR Spectroscopy

NMR spectra were recorded on a Bruker AMX-300 spectrometer, using sample tubes 5 mm in diameter and 3-(trimethylsilyl)-1-propanesulphonic acid (DSS) as internal reference. All chemical shifts for ^{1}H (δ_H) and ^{13}C (δ_C) are given in ppm. The solutions in D_2O were stabilized at pD 7.4 (p$D = -\log [D^+]$) by using a 0.5 M phosphate buffer. ^{13}C multiplicities were determined by using the distortionless enhancement bipolarization transfer (DEPT) method [33], and ^{13}C and ^{1}H correlations from two-dimensional heteronuclear measurements (H,C-COSY) [34].

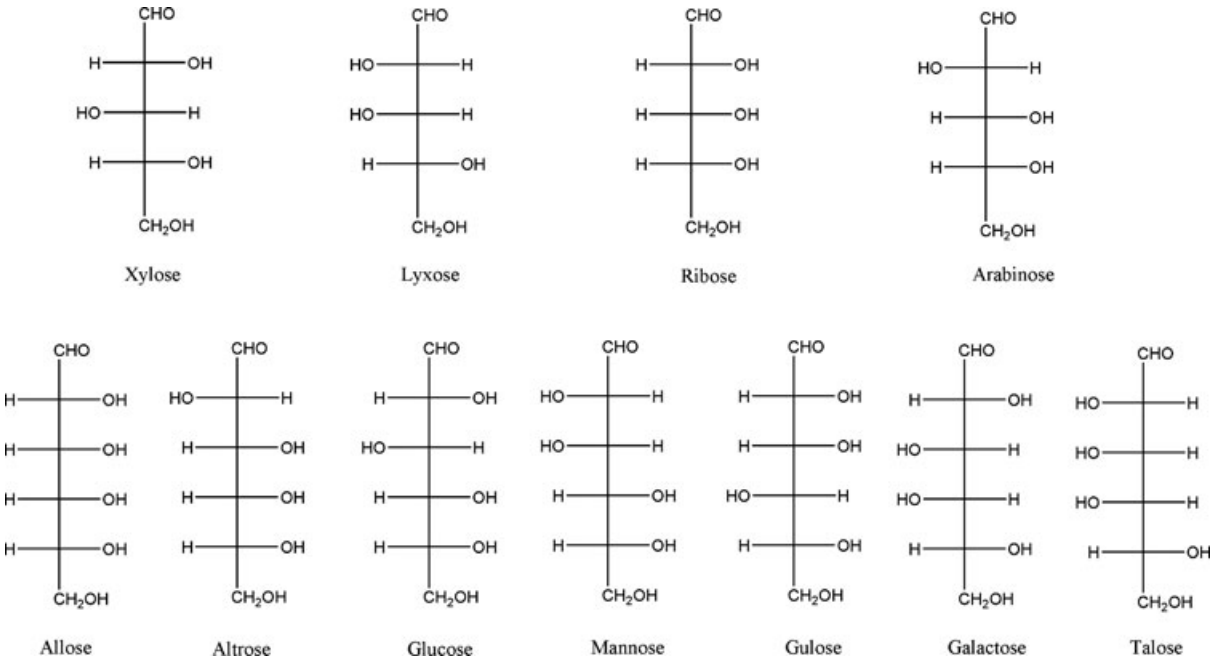

Structural formulae 1

LC–MS

Mass analyses were performed on an Agilent 1110 Series LC–MS instrument. The mobile phase was 5 mM ammonium acetate at pH 6.0—NH_4OAc initiates the ionization for MSD detection—and circulated at a flow-rate of 0.3 mL/min. The mass spectra for the isolated compounds were obtained by using a columnless flow injection analysis (FIA). No Schiff base for the hexoses was isolated; therefore, their mass spectra were obtained by injecting the reaction mixture through a Tracer Excel 120 ODSB column (25×0.46 cm, 5 μm). Mass spectral detection of the compounds was done by using an electrospray ionization interface and a quadrupole mass analyzer. The mobile phase was nebulized into an electrospray mass analyzer by using gaseous nitrogen at 350°C at a flow-rate of 13 mL/min. The detector was used to count positive ions in the scan mode over the m/z range 100–800. A nebulization pressure of 415.6 kPa, a fragmentor voltage of 80 V, and a capillary voltage of 3000 V were used.

Isolation and Identification of Products

A volume of 30 mL of each reaction mixture (0.2 M in carbohydrate, 0.005 M in pyridoxamine, and 0.5 M in phosphate buffer at pH 7.4) was heated at 37°C. Aliquots of 10 mL were collected at different times for each carbohydrate—when the concentration of the target analytes was maximum. In a subsequent step, the different compounds present in the solutions were isolated by liquid chromatography and freeze-dried. The resulting residues were characterized spectroscopically.

***3,3′,4,4′,5,6-Hexahydro-5′,6-bis(hydroxymethyl)-8′-methylspiro[pyran-2,2′-pyrido[4,3-e][1,3]oxazine]-3,4,5-triol* (5).** The chromatograms obtained for the reaction mixtures of pyridoxamine with hexoses exhibited a signal at t_R 20.3 min (Fig. 1). This compound was previously isolated, and its spectroscopic signals were found to coincide with those of **5**, which was characterized in previous work [32] (see Table I).

***2-[(3-Hydroxy-5-(hydroxymethyl)-2-methylpyridin-4-yl)methylamino]acetic Acid* (7).** After a reaction time of 30 days, an aliquot of the reaction mixture of D-lyxose and pyridoxamine was purified by HPLC to obtain **7**. HPLC: t_R 13.6 min (Fig. 2). For ^1H and ^{13}C NMR data, see Table I. EI–MS: 227.1 ($[M+H]^+$). The signals for ^{13}C in the CH_2-C(3′) group of the isolated compound were shifted downfield relative to compound **2** (δ(C) 38.9 ppm in **2** versus 46.4 ppm in **7**). The ^1H and ^{13}C chemical shifts of the other signals for the pyridine ring were similar to those obtained for compound **2**. Based on the DEPT and H,C-COSY results, C(1) in compound **7** is a secondary carbon the signal for which is shifted upfield relative to the tertiary C(1) atom in **1** (δ(C) is 94.9 ppm for **1** and 51.0 ppm for **7**). Also, C(2) in compound **7** belongs to a carbonyl group since its ^{13}C signal is shifted

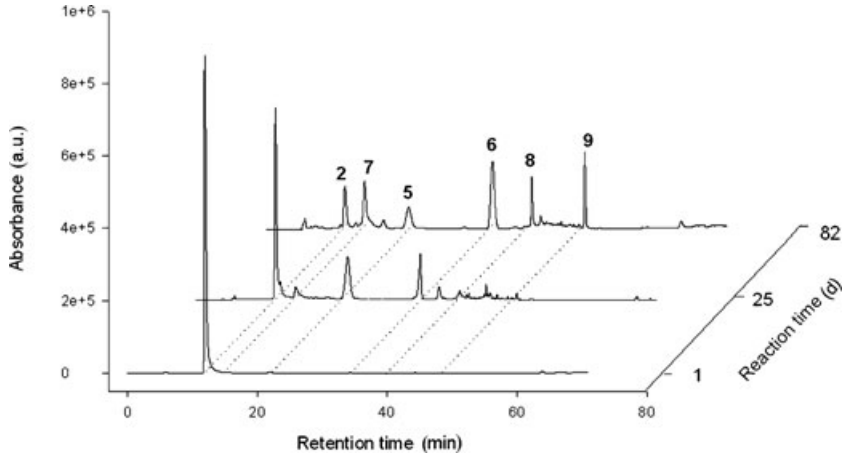

Figure 1 Time-dependent HPLC chromatograms for the reaction between 0.005 M pyridoxamine (**2**) and 0.2 M D-allose in phosphate-buffered aqueous solutions at pH 7.4 at 37°C. UV/Vis detection at 321 nm. For compounds structures, see Scheme 2.

downfield (δ(C) is 74.3 ppm for **1** and 174.2 ppm for **7**). Based on these results, the structure of **7** must coincide with that shown in Scheme 2, which was previously proposed by Glomb and Pfahler for the product of the reaction between pyridoxamine and glyoxal [35].

***Compound* 10.** After a reaction time of 3.5 days, an aliquot of the reaction mixture of D-talose and pyridoxamine was purified by HPLC (t_R 44.6 min; Fig. 3) to obtain compound **10**. Its ^{1}H and ^{13}C NMR data are shown in Table I. EI–MS: 491.1 ($[M + 2H]^+$). The ^{13}C signals for the CH_2-C(3′) group in this compound were shifted downfield relative to compound **2** (δ(C) is 38.9 ppm for **2** and 57.3 ppm for **10**) by the effect of the primary amino group in pyridoxamine becoming a tertiary group in **10**. The ^{1}H and ^{13}C shifts of the other signals for the pyridine ring are essentially similar to those for compound **2**. Based on the DEPT and H,C-COSY results, atoms C(1) and C(7) in compound **10** are quaternary atoms with downfield-shifted signals relative to the tertiary C(1) atom in compound **1** (δ(C) is 94.9 ppm for **1**, and 100.2 and 100.1 ppm for C(1) and C(7), respectively, in **10**). These results suggest that compound **10** results from condensation of pyridoxamine with two aldose molecules. A solution of the isolated compound (**10** in 0.5 M phosphate buffer at pH 7.4) was heated at 37°C. After 5 days of

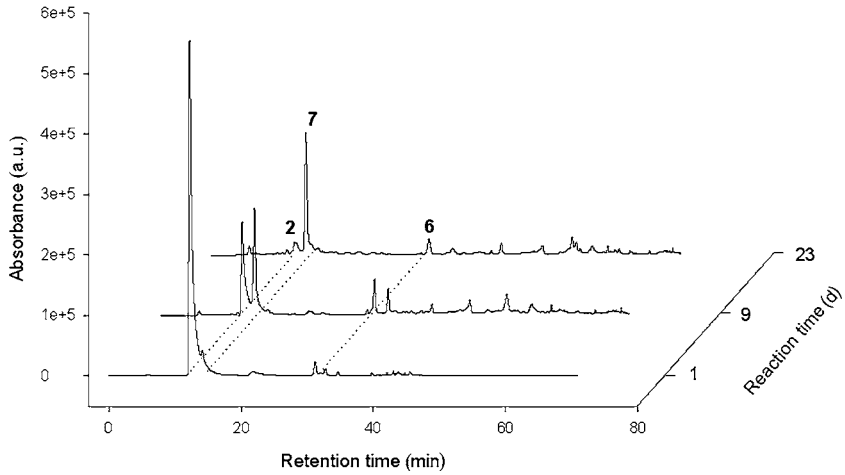

Figure 2 Time-dependent HPLC chromatograms for the reaction between 0.005 M pyridoxamine (**2**) and 0.2 M D-lyxose in phosphate-buffered aqueous solutions at pH 7.4 at 37°C. UV/Vis detection at 321 nm. For compound structures, see Scheme 2.

Table I ^{1}H- and ^{13}C-NMR Data of Compounds **1, 2, 5, 6, 7, 8, 9**, and **10** (at 300 MHz in D_2O; δ in ppm)

	1[d]		**2**		**5**[d]		**6**[a]		**7**		**8**		**9**		**10**	
	^{1}H[b]	^{13}C	^{1}H	^{13}C	^{1}H[b]	^{13}C	^{1}H	^{13}C	^{1}H	^{13}C	^{1}H	^{13}C	^{1}H	^{13}C	^{1}H[b]	^{13}C
C(1′)	–	–	–	135.2	–	133.8	–	139.4	–	133.8	–	138.3	–	**^{13}C**	–	134.9
Me-C(1′)	–	–	2.48	17.8	2.52	17.5	2.53	17.3	2.51	17.4	2.57	18.3	2.58	136.3	2.56	17.1
C(2′)	–	–	–	165.5	–	165.4	–	160.1	–	165.5	–	163.2	–	19.6	–	161.5
C(3′)	–	–	–	138.5	–	138.8	–	147.6	–	138.9	–	141.5	–	175.8	–	138.8
CH_2-C(3′)	–	–	4.31	38.9	4.46	47.5	–	–	4.42	46.4	4.85	58.8	–	157.1	4.40	57.3
HOC-C(3′)	–	–	–	–	–	–	6.62	101.7	–	–	–	–	–	–	–	–
HOOC-C(3′)	–	–	–	–	–	–	–	–	–	–	–	–	–	–	–	–
C(4′)	–	–	–	147.5	–	147.1	–	141.1	–	147.2	–	147.0	–	208.9	–	–
CH_2-C(4′)	–	–	4.73	61.7	4.73	61.4	5-6[c]	72.5	4.72	61.4	4.79	61.6	4.81	149.9	4.75	61.1
H-C(5′)	–	–	7.74	126.1	7.72	125.7	7.74	121.1	7.70	125.7	7.92	127.8	7.81	63.3	7.90	128.6
H-C(1)	5.21	94.9	–	–	–	97.9	–	–	–	–	–	–	–	130.8	–	100.2
H_2-C(1)	–	–	–	–	–	–	–	–	3.63	51.0	–	–	–	–	–	–
H-C(2)	3.51	74.3	–	–	3.75	71.6	–	–	–	–	–	–	–	–	4.15	72.3
HOO-C(2)	–	–	–	–	–	–	–	–	–	174.2	–	–	–	–	–	–
H-C(3)	3.69	75.6	–	–	3.92	72.2	–	–	–	–	–	–	–	–	3.6	68.7
H-C(4)	3.39	72.5	–	–	3.33	71.3	–	–	–	–	–	–	–	–	3.7	72.7
H-C(5)	3.81	74.3	–	–	4.05	71.6	–	–	–	–	–	–	–	–	4.05	72.3
CH_2-C(5)	3.81	63.5	–	–	4.05	66.5	–	–	–	–	–	–	–	–	3.82	65.2
C(7)	–	–	–	–	–	–	–	–	–	–	–	–	–	–	–	100.1
H-C(8)	–	–	–	–	–	–	–	–	–	–	–	–	–	–	3.93	74.4
H-C(9)	–	–	–	–	–	–	–	–	–	–	–	–	–	–	3.98	72.3
H-C(10)	–	–	–	–	–	–	–	–	–	–	–	–	–	–	3.86	72.5
H-C(11)	–	–	–	–	–	–	–	–	–	–	–	–	–	–	3.9	72.8
CH_2-C(11)	–	–	–	–	–	–	–	–	–	–	–	–	–	–	3.85	65.6

[a] The data for compound **6** correspond to its hydrated form, which was the major one at the working pH [49].

[b] The ^{1}H coupling constants for compounds **1, 5** and **10** could not be determined.

[c] This signal could not be distinguished as it was overlapped with the solvent peak. Its presence was confirmed by DEPT and H,C-COSY analysis.

[d] The chemical shifts for compounds **1** and **5** were taken from a previous paper [32].

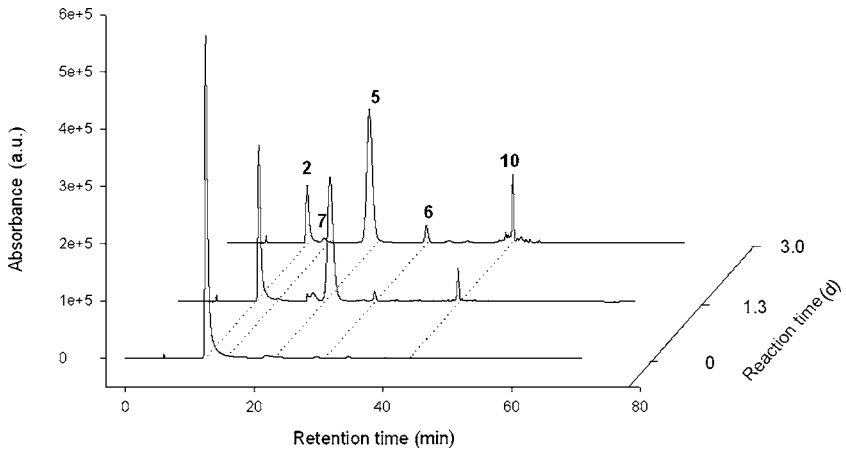

Figure 3 Time-dependent HPLC chromatograms for the reaction between 0.005 M pyridoxamine (**2**) and 0.2 M D-talose in phosphate-buffered aqueous solutions at pH 7.4 at 37°C. UV/Vis detection at 321 nm. For compounds structures, see Scheme 2.

incubation, the solution was analyzed by column LC–MS. The chromatogram obtained exhibited a signal at t_R 44.6 min corresponding to **10** in addition to one at t_R 20.3 min corresponding to **5**. The mass spectrum included a signal at m/z 219.0 corresponding to $[M+K]^+$ for D-talose. The areas of the chromatographic peaks leveled off after 3 days of incubation, suggesting that the k_{12}/k_{-12} equilibrium had been established. One can therefore reasonably assume that compound **10** is formed by condensation of **5** with another sugar molecule.

3-Hydroxy-5-(hydroxymethyl)-2-methylpyridine-4-carbaldehyde (6), 4,5-Bis-(hydroxymethyl)-2-methylpyridin-3-ol (8), and 3-Hydroxy-5-(hydroxymethyl)2-methylpyridine-4-carboxylic acid (9). After a reaction time of 100 days, an aliquot of the reaction mixture of pyridoxamine and D-mannose was purified by HPLC to obtain compounds **6, 8**, and **9**, and the structures of which were confirmed by comparing their NMR and EI–MS data with those for commercial samples. HPLC: t_R 32.2, 40.6, and 47.4 min for **6, 8**, and **9**, respectively (see Fig. 1). ^{1}H and ^{13}C NMR: see Table I. EI–MS: 168.0 ($[M+H]^+$) for **6**, 170.0 ($[M+H]^+$) for **8**, and 184.0 ($[M+H]^+$) for **9**.

5-(Hydroxymethyl)-2-methyl-4-{[(2,3,4,5,6-pentahydroxyhexylidene)amino]methyl}pyridin-3-ol (3). A reaction mixture containing 0.4 M hexose (**1**) and 0.02 M pyridoxamine (**2**) in 0.5 M phosphate buffer at pH 7.4 at 37°C was used in order to increase the concentration of Schiff base obtained. The solution exhibited substantial accumulation of compound **3** after 3–8 days. HPLC: t_R 44.2 min. EI–MS: 331.1 ($[M+H]^+$). The Schiff bases could not be characterized by NMR spectroscopy since, as found in previous work [32], they decomposed rapidly.

Kinetic Rate Constants

Rate constants were determined by using the kinetic data processing software GIT [36,37], which performs numerical integration of the differential equations corresponding to a given kinetic scheme.

Determination of Schiff Base Formation (k_3)

Based on Scheme 2, the following kinetic equation is proposed under the operating conditions used to examine the reaction between compounds **1** and **2** (in a 40:1 ratio):

$$\frac{-\mathrm{d}[\mathbf{2b}]}{\mathrm{d}t} = k_3[\mathbf{1b}]\,[\mathbf{2b}] - k_{-3}[\mathbf{3}] \tag{1}$$

Under such conditions, the following steady-state approximation can be used for compound **3**:

$$\frac{\mathrm{d}[\mathbf{3}]}{\mathrm{d}t} = k_3[\mathbf{1b}][\mathbf{2b}] - k_{-3}[\mathbf{3}] - k_4[\mathbf{3}] - k_5[\mathbf{3}] - k_6[\mathbf{3}] = 0 \tag{2}$$

from which it follows that

$$[\mathbf{3}] = \frac{k_3[\mathbf{1b}]\ [\mathbf{2b}]}{k_{-3}+k_4+k_5+k_6} \tag{3}$$

Substitution of Eq. (3) into (1) yields

$$\frac{-\mathrm{d}[\mathbf{2b}]}{\mathrm{d}t} = k_3[\mathbf{1b}][\mathbf{2b}] - k_{-3}\frac{k_3[\mathbf{1b}][\mathbf{2b}]}{k_{-3}+k_4+k_5+k_6} \tag{4}$$

which can be rearranged to

$$\frac{-\mathrm{d}[\mathbf{2b}]}{\mathrm{d}t} = \frac{k_3\,(k_4+k_5+k_6)}{k_{-3}+k_4+k_5+k_6}[\mathbf{1b}]\,[\mathbf{2b}] \tag{5}$$

Based on the equilibria between forms **1a** and **1b** in glucose and forms **2a** and **2b** in pyridoxamine,

$$K_1 = \frac{[\mathbf{1b}]}{[\mathbf{1a}]} \tag{6}$$

$$K_2 = \frac{[\mathbf{2b}]}{[\mathbf{2a}]} \tag{7}$$

substitution of which into Eq. (5) yields

$$\frac{-\mathrm{d}[\mathbf{2b}]}{\mathrm{d}t} = \frac{k_3(k_4+k_5+k_6)}{k_{-3}+k_4+k_5+k_6}K_1K_2[\mathbf{1a}][\mathbf{2a}] \tag{8}$$

Since compound **1** is present in overstoichiometric amounts in the reaction medium, its concentration can be assumed to remain constant. By collecting all constant terms in Eq. (8), one can define a new constant k_r such that

$$k_r = \frac{k_3\,(k_4+k_5+k_6)}{k_{-3}+k_4+k_5+k_6}K_1K_2[\mathbf{1a}] \tag{9}$$

substitution of which into Eq. (8) yields

$$\frac{-\mathrm{d}[\mathbf{2b}]}{\mathrm{d}t} = k_r[\mathbf{2a}] \tag{10}$$

Taking into account that the different tautomers of pyridoxamine are in mutual equilibrium, substituting [**2b**]

as a function of [**2a**] into Eq. (10) yields

$$\frac{-\mathrm{d}[\mathbf{2a}]}{\mathrm{d}t} = k_r[\mathbf{2a}] \tag{11}$$

which can be integrated to

$$\ln \frac{[\mathbf{2a}]}{[\mathbf{2a}]_0} = -k_r t \tag{12}$$

A plot of ln [**2**] as a function of time was linear throughout. This allowed us to determine the pseudo-first-order rate constants k_r from the experimental temporal variation of the concentration of compound **2**, using Eq. (12). Also, Eq. (9) allowed us to determine the formation constant for the Schiff base, k_3, from the initial concentration of **1** in the reaction mixture, the equilibrium constants K_1 and K_2, and the constants k_{-3}, k_4, k_5, and k_6.

Theoretical Methodology

Initially, the conformational study was based on the Monte Carlo simulation with the AMBER* force field [38], and the continuum method for simulating the aqueous phase as implemented in the software MacroModel v. 6.0. [39]. We selected those conformational structures with a difference of less than 15 kJ/mol in the overall energy minimum among those obtained in the simulation. The geometry of each selected structure was optimized semiempirically by using the AM1 Hamiltonian [40] included in the software AMPAC v. 5.0. [41]. The solvent effect was included in the calculations by using the continuum method COSMO [42] as implemented in AMPAC. Subsequently, the three structures of minimum energy for each sugar were selected and reoptimized by using the DFT methodology in conjunction with the B3LYP functional [43] and the bases in the 6-31+G* set including the polarized and diffuse basis functions required for these specific computations on our system [44]. Solvent effects were considered by using the Onsager model [45] in order to optimize structures in terms of geometry and energy. The resulting structures were then energy relaxed by using Tomasi's polarizable continuum model (PCM) [46] without geometry optimization. Charges were calculated by the NBO analysis [47]. DFT computations were done by using the software Gaussian98 [48] on a Silicon Graphics Origin 200 R-10000 computer.

RESULTS AND DISCUSSION

Interaction Between Pyridoxamine and Pentoses

Figure 2 shows the temporal variation of the chromatographic signals during the reaction between pyridoxamine and D-lyxose. The assignation of chromatographic signals to chemical structures is described in the Experimental section, and the compounds corresponding to each number are shown in Scheme 2. The initial chromatogram consisted essentially of a signal corresponding to pyridoxamine (**2**) (t_R 11.4 min). After 9 days of reaction, the chromatogram included several signals including the previous one for pyridoxamine, one at t_R 13.6 min corresponding to compound **7**, another at t_R 32.3 min suggesting the presence of pyridoxal (**6**) and several other, minor signals corresponding to compounds that could not be isolated. After 23 days, the signal for compound **7** was strongly increased at the expense of that for compound **2**.

The chromatograms for the reactions of pyridoxamine with other pentoses (D-arabinose, D-ribose, and D-xylose) coincided with those for its reaction with D-lyxose, which suggests that the interaction between pyridoxamine and a pentose involves the same mechanism and gives **6** and **7** as major compounds.

Scheme 2 with $R = \mathrm{H}$ illustrates the kinetics of the reactions between pyridoxamine and pentoses. Like all other aldoses, dissolved pentoses exhibit a tautomeric equilibrium between their extended forms and various cyclic forms that are defined by a constant K_1. Also, pyridoxamine exhibits an equilibrium between its tautomers with a free amino group and those with a protonated group (K_2). First, the primary amino group in pyridoxamine (**2b**) performs a nucleophilic attack on the carbonyl group of the pentose in its extended form (**1b**). Condensation of **1** and **2** gives a Schiff base that exhibits no signal in the chromatogram but undergoes two different processes, namely (a) decomposition, by transamination [50], into compound **6** and an alditol derivative and (b) rearrangement into an Amadori compound (**4**) [5] that can in turn decompose by cleavage of the C(2)–C(3) bond to give compound **7** and a carboxylic acid by means of an oxidative mechanism. This bond cleavage reaction has previously been put forward by other authors to account for the formation of CML through interaction between sugars and lysine residues in proteins [15,51].

Interaction Between Pyridoxamine and Hexoses

Figure 1 shows the temporal variation of the chromatogram for the reaction between pyridoxamine and

D-allose. The assignation of chromatographic signals to chemical structures is described in the Experimental section. The first chromatogram exhibited a single signal that corresponded to pyridoxamine (**2**) (t_R 11.4 min). That obtained after 25 days of reaction contained several major signals, including that for pyridoxamine, another for compound **5** (t_R 20.6 min), and a third for compound **6** (t_R 32.3 min), in addition to three minor signals for **7** (t_R 13.6 min), **8** (t_R 40.5 min), and **9** (t_R 47.2 min). Finally, the chromatogram obtained at a long-reaction time exhibited significantly decreased signals for compounds **2** and **5**, and markedly increased signals for **6–9**.

The chromatograms obtained for the reactions of pyridoxamine with D-altrose, D-galactose, and D-mannose were qualitatively consistent with those for its reaction with D-allose. This suggests that the reactions between pyridoxamine and the previous hexoses take place via the same mechanism—the end-products are identical in any case. In previous work, the reaction between pyridoxamine and D-glucose was found to give the same end-products except **7**, which was not detected [32].

We also studied the reactions of pyridoxamine with D-talose and D-gulose; the chromatograms for which differed from those obtained with the other hexoses. Figure 3 shows the temporal variation of the chromatographic signals during the reaction between pyridoxamine and D-talose. The initial chromatogram exhibited a single signal corresponding to pyridoxamine (**2**) (t_R 11.4 min). The chromatogram obtained after 1 day of reaction was consistent with partial reaction of **2** and included three major signals corresponding to compounds **5** (t_R 20.6 min), **6** (t_R 32.3 min), and **10** (t_R 44.4 min). That obtained after 3 days of reaction exhibited a further decreased signal for compound **2** and increased signals for **5, 6**, and **10**, in addition to a new one corresponding to **7**. The chromatograms for the reaction between pyridoxamine and D-gulose were similar to those for the previous reaction.

Scheme 2 with $R = CH_2OH$ illustrates the kinetics of the reactions between pyridoxamine and hexoses. Initially, the carbonyl group in the extended form of the hexose (**1b**) undergoes a nucleophilic attack from the primary amino group in pyridoxamine (**2b**). Then, condensation of **1** and **2** gives compound **3**, which is a Schiff base. Figures 1 and 3 show no trace of this compound because the reactant concentrations used precluded its accumulation. The Schiff base **3** evolved in three different ways depending on the nature of the particular hexose, namely (a) decomposition, by transamination, into compound **6** and an alditol derivative; (b) a double internal cyclization and the result being compound **5**, that was previously isolated and characterized by our group [32]—the amount of **5** obtained was greater in the sugars with a minor extended form (viz., D-glucose and D-mannose); and (c) rearrangement into an Amadori compound (**4**).

Compound **5** decomposes into **6, 8**, and **9** as major products; compound **9**, however, can also form by oxidation of **6** [52]. Compound **7**, which comes from **4**, is obtained in a higher proportion from the hexoses possessing a higher proportion of the aldehyde form (viz., D-allose, D-altrose, and D-galactose). On the other hand, compounds **8** and **9** are obtained in higher proportions from hexoses with lower proportions of their free aldehyde forms (viz., D-glucose and D-mannose).

The reactions of D-gulose and D-talose with pyridoxamine give compound **10**, which is formed by the condensation of the secondary amino group in **5** with another sugar molecule, followed by internal cyclization between the hydroxyl group in C(5)-CH_2OH and C(1) in the new sugar added (C(7) in **10**); this, in turn, undergoes cyclization via the OH-C(11) group by a similar mechanism to that proposed for the formation of **5** [32]. Therefore, in reacting with D-gulose and D-talose, pyridoxamine can scavenge two carbohydrate molecules per vitamer molecule.

Determination of Rate Constants

Quantitative kinetic determinations were done by examining the temporal variation of the chromatographic signals. The temporal variation of the concentrations of the reaction products was established by fitting changes in chromatographic peak area to the following equation:

$$[A_2]_0 = c_2A_2 + c_5A_5 + c_6A_6 + c_7A_7 + c_8A_8 + c_9A_9 + c_{10}A_{10} \quad (13)$$

where A_i is the peak area of the signal at 321 nm for each species, $[A_2]_0$ is the initial pyridoxamine concentration, and c_i are constants of proportionality between areas and concentrations. Commercially available **2, 6, 8**, and **9** were used to determine the following c_i values from a calibration plot: $c_2 = 0.044 \pm 0.004$, $c_6 = 0.091 \pm 0.003$, $c_8 = 0.111 \pm 0.005$, and $c_9 = 0.132 \pm 0.002$. Parameters c_5, c_7, and c_{10} were determined by using the software SigmaPlot 9.00 [53] to perform a nonlinear multivariate regression of Eq. (13). The parameter values thus obtained were $c_5 = 0.059 \pm 0.006$, $c_7 = 0.177 \pm 0.007$, and $c_{10} = 0.266 \pm 0.006$.

Kinetic constants were calculated by fitting the experimental temporal concentration changes for each compound to Scheme 2, using numerical integration

Table II Kinetic Constants at 37°C as Obtained by HPLC for a Reaction Mixture of 0.2M **1** and 0.005M **2** in 0.5M Phosphate Buffer (pH 7.4)

Aldose	$K_1 \times 10^5$ [a]	$k_3 \times 10^{-4}$ ($M^{-1}\ h^{-1}$) [c]	k_{-3} (h^{-1})	$k_4 \times 10^2$ (h^{-1})	$k_5 \times 10^2$ (h^{-1})	k_6 (h^{-1})	$k_{10} \times 10^{-3}$ (h^{-1})	$k_{12} \times 10^{-2}$ ($M^{-1}\ h^{-1}$)	$k_{-12} \times 10^2$ (h^{-1})	$k_d \times 10^4$ (h^{-1})
Altrose	36	5.9 (5.8)	3.4	2.1	7.2	–	0.87	–	–	98
Arabinose	33	5.5 (6.0)	25	51	–	0.34	1.4	–	–	–
Galactose	17	5.7 (5.5)	3.0	0.96	9.1	–	1.0	–	–	96
Allose	11	9.6 (9.9)	1.5	1.9	5.2	0.036	1.7	–	–	123
Glucose [b]	2.2	9.2 (10)	16	–	110	–	–	–	–	27
Lyxose	25	9.7 (10)	17	57	–	0.43	1.4	–	–	–
Manose	5.3	9.0 (9.7)	13	4.2	83	–	2.1	–	–	37
Xylose	16	9.9 (10)	13	49	–	0.32	2.5	–	–	–
Gulose	19	13 (14)	20	3.5	133	–	1.8	5.7	4.5	9.6
Ribose	47	14 (14)	8.9	30	–	0.44	1.7	–	–	–
Talose	33	13 (13)	8.3	1.9	110	–	1.4	6.1	6.9	17

[a] The K_1 values for the sugars were those reported by Miller [54].
[b] The values for the reaction with D-glucose were taken from a previous paper [32].
[c] The values in brackets were calculated from the concentration decrease in **2** with time (see the Experimental section).

of the differential equations for the scheme with the aid of the software GIT [36,37].

At pH 7.4, the proportion of aldose with a linearly arranged carbonyl group (**1b**) required to react was very low [54]. Table II lists the mutarotation constant of each aldose used in the fitting (K_1). The tautomeric constant for pyridoxamine, K_2, was taken to be 3.5×10^{-2}, which was determined in previous work [55] and was used in similar studies [32]. Finally, the pyridoxal oxidation constant, k_{11}, was taken to be $(2.6 \pm 0.2) \times 10^{-4}\ h^{-1}$, which was also determined in previous work [32].

The final concentrations of pyridoxal, pyridoxine and 4-pyridoxic acid in the reactions of pyridoxamine with the hexoses were all very low; this precluded accurate estimation of individual formation constants and led us to calculate a general decomposition constant for compound **5**: $k_d = k_7 + k_8 + k_9$. Figure 4 shows the fitting of the experimental data for the reactions of pyridoxamine with D-talose and D-xylose to Scheme 2, and Table II presents the best constant values obtained in the fitting.

Kinetic constant k_3 was also estimated from the concentration change of compound **2** as a function of time (see the Experimental section). The results (Table II) were consistent with the k_3 values obtained by fitting. Thus, k_3 ranged from 5.5×10^4 to $14 \times 10^4\ M^{-1}\ h^{-1}$. The values for D-altrose, D-arabinose, and D-galactose were similar to one another and smaller than those for D-allose, D-glucose, D-mannose, D-lyxose, and D-xylose—the k_3 values for which were in turn smaller than those for D-gulose, D-ribose, and D-talose. These results must be a consequence of the electrophilic character of the carbonyl carbon in the sugars.

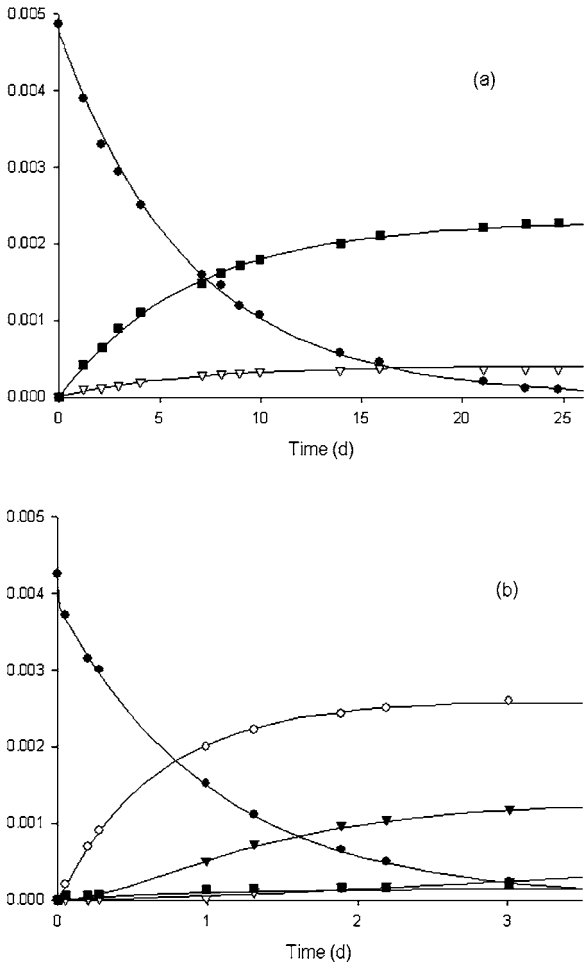

Figure 4 Time course of the decomposition of pyridoxamine (**2**) in the presence of D-xylose (a) or D-talose (b), in phosphate buffer at pH 7.4 at 37°C. (●) **2**, (○) **5**, (■) **7**, (▽) **6**, and (▼) **10**. Solid lines indicate the best theoretical fits.

Interestingly, the previous k_3 values are of the same order of magnitude as the constants for the nucleophilic attack of various amino acids on D-glucose previously obtained by other authors (viz., 60×10^3 M^{-1} h^{-1} for glycine [19], 12×10^3 M^{-1} h^{-1} for phenylalanine [20], and 15×10^3 M^{-1} h^{-1} for hemoglobin [21]). On the other hand, the reaction constants for hemoglobin with various aldoses and ketoses determined by Bunn and Higgins [22] were rather different from those obtained in this work; however, their values cannot be directly compared with ours as they failed to consider the proportions of linear carbohydrate form, pK_a for the attacking amino group and the number of terminal amino residues in hemoglobin.

The k_4 values obtained suggest that the Schiff bases formed between pentoses and pyridoxamine tend to evolve to an Amadori compound more markedly than do those formed with hexoses. The latter evolved to compound **5** by virtue of the tendency of sugars to cyclicizing (k_5).

Decomposition of the Schiff base by transamination (k_6) was only substantial in the reactions between pyridoxamine and pentoses. As can be seen from Table II, k_6 was virtually identical for all pentoses and roughly ten times smaller for D-allose.

Constant k_{10} corresponds to the oxidative degradation of compound **4** to give compound **7**. The k_{10} values obtained were virtually identical for all aldoses. Also, k_{12} and k_{-12} were virtually identical for D-gulose and D-talose.

Theoretical Calculations

As noted earlier, the disparate reactivity of the sugars toward the nucleophile (pyridoxamine in our case) must be a result of a disparate electrophilic character of the carbonyl carbon, which in turn must be related to its electron density. In order to obtain more accurate information in this respect, we calculated the net NBO charge on the carbonyl group of each sugar by using the density functional theory (DFT) as described in the Experimental section.

Figure 5 shows the variation of the formation constant for the Schiff base (k_3) for each sugar with the net NBO charge on the carbonyl carbon in the sugars. The results reveal a correlation between k_3 and the net NBO charge on the carbonyl carbon, C(1), in the extended form of each sugar. The fact that D-gulose and D-talose possess a much higher net charge than the other hexoses may explain why these are the only two sugars giving compound **10**—the electrophilic character of the carbonyl carbon in the other sugars may not be high enough to react with the secondary amino group in **5**. The absence of compound **10** among the reaction products for D-ribose (a sugar with a similar electron density) is quite consistent with the previously noted fact that the Schiff bases of the pentoses evolved to an Amadori compound (**4**) rather than to the tricyclic compound **5**.

Figure 6 shows the three structures of minimum energy identified by using the theoretical methodology described in the Experimental section. The results suggest that the variation of the electron density on the carbonyl carbon in each aldose, C(1), must be related to the hydrogen bond network formed by the linear forms of the sugars.

In structure A, which corresponds to the energy minimum for D-gulose, the oxygen atom in the carbonyl group forms a hydrogen bond with the hydroxyl group on C(2) that in turn is a member of a

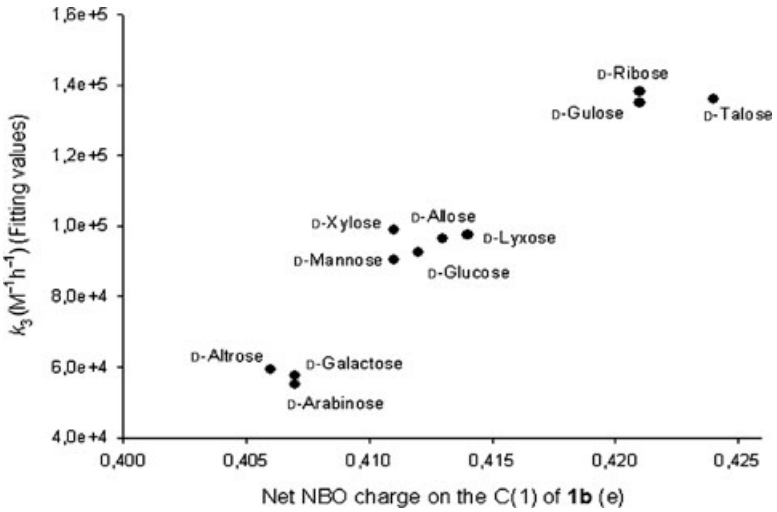

Figure 5 Relationship between the rate constant of condensation of monosaccharides with pyridoxamine (k_3) and NBO charges on the carbonyl group of the reducing form of hexoses and pentoses.

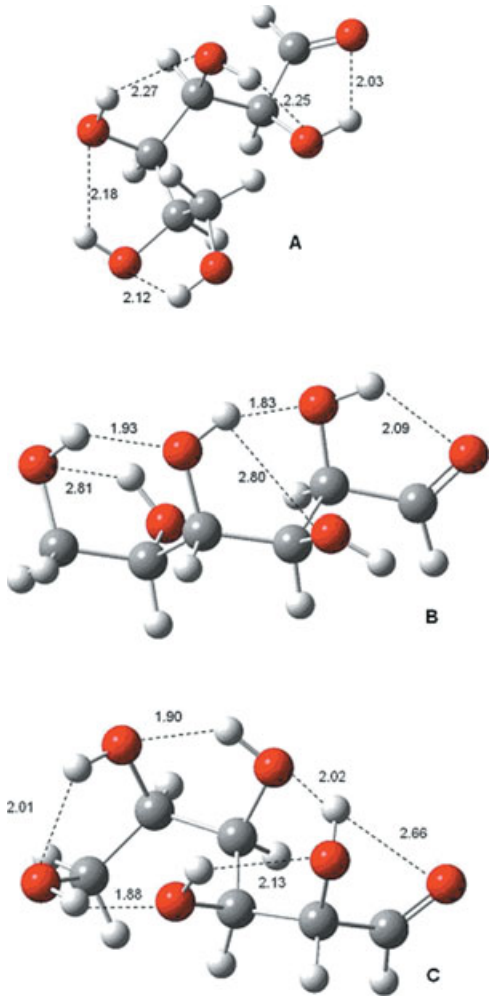

Figure 6 Structures of D-gulose (A), D-mannose (B), and D-galactose (C). O–H distances are given in angstroms. [Color figure can be viewed in the online issue, which is available at www.interscience.wiley.com.]

network of four hydrogen bonds with the other hydroxyl groups in the aldose which reduce the electron density on the carbonyl carbon. In structure B, which represents the minimum for D-mannose, the carbonyl oxygen is also a part of a hydrogen bond with a hydroxyl group on C(2); however, such a group forms a network of only two hydrogen bonds with the other hydroxyls, so the electron density on the carbonyl carbon is less markedly reduced than in the previous case. Finally, structure C corresponds to the energy minimum for D-galactose. As can be seen, the carbonyl oxygen forms no hydrogen bond with any hydroxyl group on the hydrocarbon chain; as a result, this structure exhibits the lowest net NBO charge on the carbonyl carbon.

CONCLUSIONS

The results obtained in this work for the reactions of pyridoxamine with various sugars—hexoses and pentoses—reveal marked differences in their mechanisms depending on the nature of the carbohydrate. Initially, both types of sugars form a Schiff base by condensation of the amino group in the pyridine compound with the carbonyl group in the linear form of the sugar (**1b** in Scheme 2). The calculated net NBO charge on the carbonyl carbon clearly indicates that the reactivity of the sugars (k_3) is related to such electronic density, which is determined by the network of intramolecular hydrogen bonds formed with the carbonyl oxygen but independent of the length of the sugar chain. Thus, D-gulose, D-ribose, and D-talose, which possess a net NBO charge on the carbonyl carbon in the region of 0.423 e, have k_3 values one order of magnitude greater than those for D-altrose, D-galactose, and D-arabinose, the NBO charge on the carbonyl carbon of which is 0.407 e.

The Schiff bases can evolve in various ways depending on the length of the sugar chain. In hexoses, the preferential reaction is the formation of a highly stable tricyclic compound (**5**) by cyclization of the carbohydrate portion of the Schiff base. In pentoses, however, the reaction takes place mainly by proton rearrangement and gives a highly unstable Amadori compound (k_4) that is hydrolyzed to two new carboxylic acids.

The Schiff base formed in the reactions of pyridoxamine with pentoses also decomposes, by transamination (k_6), into pyridoxal (**6**). The presence of pyridoxal in the reaction mixture suggests that the transamination reaction may contribute to the inhibitory action of pyridoxamine on AGEs, particularly in those reactions involving pentoses. In hexoses, however, the transamination reaction is insubstantial as their Schiff bases evolve largely to compound **5**. Even so, their reaction products included pyridoxal (**6**) and pyridoxine (**8**) resulting from the decomposition of **5**, and these compounds can further inhibit glycation via previously reported mechanisms [25,28].

The reactions of pyridoxamine with D-talose and D-gulose—two hexoses with a low-electron density on the carbonyl carbon—give compound **10**; therefore, each molecule of pyridoxamine must be able to scavenge two hexose molecules with a low charge on their carbonyl carbon.

In any case, the k_3 values obtained for the reactions of aldoses with pyridoxamine, and the fact that no new glycating carbonyl groups are produced, confirm the ability of pyridoxamine to inhibit protein glycation by scavenging glycating carbonyl groups from aldoses.

Altering its molecular structure by increasing the nucleophilic character of the amino group and/or displacing the equilibrium to its deprotonated form should enhance its inhibitory power.

BIBLIOGRAPHY

1. Maillard, L. C. C R Acad Sci 1912, 154, 66–68.
2. Sattler, L.; Zerban, F. W. Int Eng Chem 1949, 41, 1401–1407.
3. Ledl, F.; Schleicher, E. Angew Chem, Int Ed Engl 1990, 29, 565–594.
4. Monnier, V. M. Arch Biochem Biophys 2003, 419(1), 1–15.
5. Yaylayan, V. A.; Huyghues-Despointes, A. Crit Rev Food Sci 1994, 34(4), 321–369.
6. Miyata, T.; Van Ypersele De Strihou, C; Ueda, Y.; Ichimori, K.; Inagi, R.; Onogi, H.; Ishikawa, N.; Nangaku, M.; Kurokawa, K. J Am Soc Nephrol 2002, 12, 2478–2487.
7. Prakash Reddy, V.; Obrenovich, M. E.; Atwood, C. S.; Perry, G.; Smith, M. Neurotoxin Res 2002, 4(3), 191–209.
8. Kume, S.; Takeya, M.; Mori, T.; Araki, N.; Suzuki, H.; Horiuchi, S.; Kodama, T.; Miyauchi, Y.; Takahashi, K. Am J Pathol 1995, 147, 654–667.
9. Tessier, T.; Obrenovich, M.; Monnier, V. M. J Biol Chem 1999, 274, 20796–20804.
10. Waanders, F.; Greven, W. L.; Baynes, J. W.; Thorpe, S. R.; Kramer, A. B.; Nagai, R.; Sakata, N.; Van Goor, H.; Navis, G. Nephrol Dial Transpl 2005, 20(10), 2060–2070.
11. Reihl, O.; Biemel, K. M.; Lederer, M. O.; Schwack, W. Carbohydr Res 2004, 339, 705–714.
12. Obayashi, H.; Nakano, K.; Shigeta, H.; Yamaguchi, M.; Yoshimori, K.; Fukui, M.; Fujii, M.; Kitagawa, Y.; Nakamura, N.; Nakamura, K.; Nakazawa, Y.; Ienaga, K.; Ohta, M.; Nishimura, M.; Fukui, I.; Kond M. Biochem Biophys Res Commun 1996, 226, 37–41.
13. Wells-Knecht, K. J.; Zyzak, D. V.; Litchfield, J. E.; Thorpe, S. R.; Baynes, J. W. Biochemistry 1995, 34, 3702–3709.
14. Dyer, D. G.; Blackledge, J. A.; Thorpe, S. R.; Baynes, J. W. J Biol Chem 1991, 266, 11654–11660.
15. Ahmed, M. U.; Dunn, J. A.; Walla, M. D.; Thorpe, S. R.; Baynes, J. W. J Biol Chem 1988, 263, 8816–8821.
16. Cheng, R.; Feng, Q.; Ognyan, K. A.; Ortweth, B. J. Ann NY Acad Sci 2005, 1043, 184–194.
17. Bucala, R.; Model, P.; Cerami, A. Proc Natl Acad Sci 1984, 48, 105–109.
18. Baynes, J. W.; Thorpe, S. R. Free Radic Biol Med 2000, 28(12), 1708–1716.
19. Labuza, T. P.; Baisier, W. M. J Agric Food Chem 1992, 40, 707–713.
20. Ge, S. J.; Lee, T. C. J Agric Food Chem 1997, 45, 1619–1623.
21. Bunn, H. F.; Higgins, P. J. J Biol Chem 1981, 256, 5204–5208.
22. Bunn, H. F.; Higgins, P. J. Science 1981, 213, 222–224.
23. Brownlee, M.; Vlassara, H.; Kooney, A.; Ulrich, P.; Cerami, A. Science 1986, 232, 1629–1632.
24. Hobart, L. J.; Seibel, I.; Yeargans, G. S.; Seidler, N. W. Life Sci 2004, 75, 1379–1389.
25. Culbertson, S. M.; Vassilenko, E. I.; Morrison, L. D.; Ingold, K. U. J Biol Chem 2003, 278, 38384–38394.
26. Voziyan, P. A.; Hudson, B. G. Ann NY Acad Sci 2005, 1043, 807–816.
27. Voziyan, P. A.; Metz, T. O.; Baynes, J. W.; Hudson, B. G. J Biol Chem 2002, 277, 3397–6403.
28. Booth, A. A.; Khalifah, R. G.; Hudson, B. G. Biochem Biophys Res Commun 1996, 220, 113–119.
29. Voziyan, P. A.; Hudson, B. G. Cell Mol Life Sci 2005, 62(15), 1671–1681.
30. Onorato, J. M.; Jenkins, A. J.; Thorpe, S. R.; Baynes, J. W. J Biol Chem 2000, 275, 21177–21184.
31. Khalifah, R. G.; Chen, Y.; Wassenberg, J. J. Ann NY Acad Sci 2005, 1043, 793–806.
32. Adrover, M.; Vilanova, B.; Muñoz, F.; Donoso, J. Chem Biodivers 2005, 2, 964–975.
33. Doddrell, D. M.; Pegg, D. T.; Bendall, M. R. J Magn Reson 1982, 48, 323–327.
34. Derone, A. E. Modern NMR Techniques for Chemistry Research; Pergamon Press: New York, 1987.
35. Glomb, M. A.; Pfahler, C. J Biol Chem 2001, 276, 41638–41647.
36. Stabler, R. N.; Chesick, J. P. Int J Chem Kinet 1978, 10, 461–469.
37. Weigert, F. J. Comput Chem 1987, 11, 273–280.
38. Weiner, S. J.; Kollman, P. A.; Case, D. A.; Singh, U. C.; Chio, C.; Alagona, G.; Profeta, S.; Weiner, P. J Am Chem Soc 1984, 106, 765–784.
39. Mohamadi, F.; Richards, N. G. J.; Guida, W. C.; Liskamp, R.; Caufield, C.; Chang, G.; Hendrickson, T.; Still, W. C. J Comput Chem 1990, 11, 440–467.
40. Dewar, M. J. S.; Zoebisch, E. G.; Healy, E. F.; Stewart, J. J. P. J Am Chem Soc 1985, 107, 3902–3909.
41. AMPAC v. 6.0; Semichem, Shawnee, KS, 1997.
42. Klamt, A. J. J Phys Chem 1995, 99, 2224–2235.
43. Lee, C.; Yang, W.; Parr, R. G. Phys Rev B 1988, 37, 785–789.
44. Salvà, A.; Donoso, J.; Frau, J.; Muñoz, F. J Phys Chem A 2004, 108, 11709–11714.
45. Onsager, L. J Am Chem Soc 1936, 58, 1486–1493.
46. Miertus, S.; Scrocco, E.; Tomasi, J. Chem Phys 1981, 55, 117–129.
47. Reed, A. E.; Curtiss, L. A.; Weinhold, F. Chem Rev 1988, 88, 899–926.
48. Frisch, M. J.; Trucks, G. W.; Schlegel, H. B.; Gill, P. M. W.; Johnson, B. G.; Robb, M. A.; Cheeseman, J. R.; Keith, T.; Petersson, G. A.; Montgomery, J. A.; Raghavachari, K.; Al-Laham, M. A.; Zakrzewski, V. G.; Ortiz, J. V.; Foresman, J. B.; Cioslowski, J.; Stefanov, B. B.; Nanayakkara, A.; Challacombe, M.; Peng, C. Y.;

Ayala, P. Y.; Chen, W.; Wong, M. W.; Andres, J. L.; Replogle, E. S.; Gomperts, R.; Martin, R. L.; Fox, D. J.; Binkley, J. S.; Defrees, D. J.; Baker, J.; Stewart, J. P.; HeadGordon, M.; Gonzalez, C.; Pople, J. A. Gaussian98; Gaussian, Inc.: Pittsburgh, PA, 1998.
49. Snell, E. E. Transaminases; Wiley-Interscience: New York, 1985.
50. Snell, E. E. J Am Chem Soc 1945, 67, 194–197.
51. Kasper, M.; Schieberle, P. Ann NY Acad Sci 2005, 1043, 59–62.
52. Gregory, J. F.; Kirk, J. R. J Food Sci 1978, 43, 1801–1815.
53. SigmaPlot, v. 9.00; SPSS Inc., Erkrath, Germany, 2004.
54. Dworkin, J. P.; Miller, S. L. Carbohyd Res 2000, 329, 359–365.
55. Vilanova, B.; Adrover, M.; Muñoz, F.; Donoso, J. Chem Biodivers 2004, 1, 1073–1090.